Physics Letters B 771 (2017) 385–391

Contents lists available at ScienceDirect

Physics Letters B

www.elsevier.com/locate/physletb

Evolution of nuclear structure in neutron-rich odd-Zn isotopes and isomers

C. Wraith [a,*], X.F. Yang [b,*], L. Xie [c], C. Babcock [a], J. Bieroń [d], J. Billowes [c], M.L. Bissell [b,c], K. Blaum [e], B. Cheal [a], L. Filippin [f], R.F. Garcia Ruiz [b,c], W. Gins [b], L.K. Grob [g], G. Gaigalas [h], M. Godefroid [f], C. Gorges [i], H. Heylen [b], M. Honma [j], P. Jönsson [k], S. Kaufmann [g], M. Kowalska [l], J. Krämer [i], S. Malbrunot-Ettenauer [l], R. Neugart [e,g], G. Neyens [b], W. Nörtershäuser [g,i], F. Nowacki [m], T. Otsuka [n], J. Papuga [b], R. Sánchez [o], Y. Tsunoda [p], D.T. Yordanov [q]

[a] Oliver Lodge Laboratory, Oxford Street, University of Liverpool, Liverpool, L69 7ZE, United Kingdom
[b] KU Leuven, Instituut voor Kern- en Stralingsfysica, B-3001 Leuven, Belgium
[c] School of Physics and Astronomy, The University of Manchester, Manchester, M13 9PL, United Kingdom
[d] Instytut Fizyki imienia Mariana Smoluchowskiego, Uniwersytet Jagielloński, ul. prof. Stanisława Łojasiewicza 11, Kraków, Poland
[e] Max-Plank-Institut für Kernphysik, D-69117 Heidelberg, Germany
[f] Chimie Quantique et Photophysique, Université Libre de Bruxelles, B-1050 Brussels, Belgium
[g] Institut für Kernchemie, Universität Mainz, D-55128 Mainz, Germany
[h] Institute of Theoretical Physics and Astronomy, Vilnius University, Saulėtekio av. 3, LT-10222 Vilnius, Lithuania
[i] Institut für Kernphysik, TU Darmstadt, D-64289 Darmstadt, Germany
[j] Center for Mathematical Sciences, University of Aizu, Tsuruga, Ikki-machi, Aizu-Wakamatsu, Fukushima 965-8580, Japan
[k] School of Technology, Malmö University, Sweden
[l] Experimental Physics Department, CERN, CH-1211 Geneva 23, Switzerland
[m] IPHC, IN2P3-CNRS et Université de Strasbourg, F-67037 Strasbourg, France
[n] Department of Physics, University of Tokyo, Hongo, Tokyo 113, Japan
[o] GSI Helmholtzzentrum für Schwerionenforschung, D-64291 Darmstadt, Germany
[p] Center for Nuclear Study, University of Tokyo, Hongo, Bunkyo-ku, Tokyo 113-0033, Japan
[q] Institut de Physique Nucléaire, CNRS-IN2P3, Université Paris-Sud, Université Paris-Saclay, 91406 Orsay, France

ARTICLE INFO

Article history:
Received 10 March 2017
Received in revised form 24 April 2017
Accepted 29 May 2017
Available online 1 June 2017
Editor: V. Metag

Keywords:
Zinc
Magnetic dipole moment
Quadrupole moment
Laser
Shell closure

ABSTRACT

Collinear laser spectroscopy was performed on Zn ($Z = 30$) isotopes at ISOLDE, CERN. The study of hyperfine spectra of nuclei across the Zn isotopic chain, $N = 33$–49, allowed the measurement of nuclear spins for the ground and isomeric states in odd-A neutron-rich nuclei up to $N = 50$. Exactly one long-lived (>10 ms) isomeric state has been established in each $^{69-79}$Zn isotope. The nuclear magnetic dipole moments and spectroscopic quadrupole moments are well reproduced by large-scale shell–model calculations in the f_5pg_9 and fpg_9d_5 model spaces, thus establishing the dominant term in their wave function. The magnetic moment of the intruder $I^\pi = 1/2^+$ isomer in ^{79}Zn is reproduced only if the $\nu s_{1/2}$ orbital is added to the valence space, as realized in the recently developed PFSDG-U interaction. The spin and moments of the low-lying isomeric state in ^{73}Zn suggest a strong onset of deformation at $N = 43$, while the progression towards ^{79}Zn points to the stability of the $Z = 28$ and $N = 50$ shell gaps, supporting the magicity of ^{78}Ni.

1. Introduction

Evaluating the accuracy of large-scale shell–model interactions is dependent on experimental data in regions of shell closures. For elements with $Z \approx 28$, recent experiments have aimed to shed light on nuclear structure in the neutron-rich isotopes and hence assess the reliability of shell–model predictions. This region is known for being rich in nuclear structural change, including the weak sub-shell closure at $N = 40$ observed in nickel [1] and copper [2], the development of collectivity beyond $N = 40$ in Ga isotopes [3] and the doubly magic nature of the exotic nucleus ^{78}Ni,

* Corresponding authors.
E-mail addresses: c.wraith@liverpool.ac.uk (C. Wraith), xiaofei.yang@fys.kuleuven.be (X.F. Yang).

http://dx.doi.org/10.1016/j.physletb.2017.05.085

which is an important waiting point in the astrophysical r-process [4]. These phenomena can be understood by studies of the nuclear states directly, with laser spectroscopy proving a versatile method for measuring properties of long-lived ground and isomeric states (>10 ms), such as spins, moments and mean-square charge radii. In particular, the nuclear spins and magnetic dipole moments, μ, give information on the evolution of the single particle (SP) states of nucleons within the shell–model. Additionally, the spectroscopic quadrupole moments, Q_s, provide information on the shape of the charge distribution and collectivity in the nucleus.

Isotopes of zinc have two protons outside the $Z = 28$ shell closure. In a non-interacting shell–model picture these protons occupy the $\pi p_{3/2}$ orbital. However, studies of neighbouring $_{29}$Cu and $_{31}$Ga isotopes show that the filling of the $\nu g_{9/2}$ orbital after $N = 40$ induces a reordering of the proton SP levels $p_{3/2}$ and $f_{5/2}$, and hence a ground state (g.s.) spin change induced by the tensor force [3,5]. Due to the even proton number of zinc, the effects of this predicted level reordering on the g.s. properties of odd-A Zn isotopes will be more subtle as their moments will be dominated by the unpaired neutron. The tensor interaction decreases the size of the $Z = 28$ shell gap with increasing N, as the filling of the $\nu g_{9/2}$ orbit induces a reduction of the spin–orbit splitting between the $\pi f_{7/2}$ and $\pi f_{5/2}$ levels [6]. This interaction therefore has strong implications on shell closures in this region, and most notably at closures far from stability, where the $Z = 28$ and $N = 50$ shell gaps provide information on the effectiveness of the magicity of ^{78}Ni [7,8]. Despite these predictions, mass measurements of $^{71-81}$Zn at ISOLTRAP have highlighted the persistence of the $N = 50$ shell closure at $Z = 30$ [9], while similar measurements at JYFLTRAP have indicated an increasing rigidity of the shell gap from Ga to Ni [10]. Studies at RIBF of β-decay half-lives of ^{76,77}Co, ^{79,80}Co and ^{81}Cu, and $E(4_1^+)/E(2_1^+)$ and $B(E2; 4_1^+ \rightarrow 2_1^+)/B(E2; 2_1^+ \rightarrow 0_{g.s.}^+)$ of ^{80}Zn have also pointed towards a doubly magic structure for ^{78}Ni [11,12].

In a previous publication [13] we reported the laser spectroscopy results of an isomeric state in ^{79}Zn, which was originally reported in Ref. [14]. A preliminary analysis of this system, which also displays a signature of shape coexistence, indicated the presence of an intruder $\nu s_{1/2}$ state. Here, we report for the first time a full theoretical analysis in the context of new measurements for the entire isotopic chain. The observed nuclear magnetic dipole and spectroscopic quadrupole moments are compared with large-scale shell–model calculations in different model spaces to evaluate the influence of proton excitations across $Z = 28$ and of neutrons across $N = 50$, and the evolution of nuclear structure along the isotopic chain. Additionally, this Letter establishes firmly the ground and long-lived (>10 ms) isomeric state spins of odd-A Zn isotopes from $N = 33$–49. The direct observation of their hyperfine structure (hfs) solves a long-standing discussion about the (non-)existence of several long-lived isomeric states in some of these isotopes [15–18,14].

2. Experimental method

The experiment was completed at the collinear laser spectroscopy setup COLLAPS [19] at ISOLDE, CERN. Radioactive fission fragments were produced using a thick UC_x target (45 g/cm^2) bombarded with pulses of 1.4-GeV protons. A neutron converter [20] suppressed the production of Rb isobars, which contaminate the beam purity of neutron-rich Zn isotopes. The Zn yield was selectively enhanced by a factor of 100 using the Resonant Ionization Laser-Ion Source (RILIS) [21]. Zn ions were accelerated to 30 keV and mass selected using the high-resolution separator (HRS). A gas-filled radio frequency quadrupole, ISCOOL [22], delivered cooled and bunched ions to the collinear laser spectroscopy setup, with a typical accumulation and release cycle of 200 ms. The ion beam was neutralised in-flight through a charge exchange cell (CEC) filled with Na vapour, quasi-resonantly populating the atomic metastable 4s4p $^3P_2^o$ level at 32890.3 cm^{-1}. A co-propagating laser beam was overlapped with the emerging atomic beam in order to resonantly excite the Zn atoms. A tuning potential applied prior to the neutralisation acted to Doppler-shift the laser frequency observed by the atoms, allowing a scan over the hfs resonances. The 481.1873 nm 4s4p $^3P_2^o \rightarrow$ 4s5s $^3S_1$ transition was studied using a cw frequency-doubled titanium-sapphire laser, locked to a wavelength meter with use of an interferometer which was calibrated by a stabilized HeNe laser. A mass dependent time of flight is assigned to each ion bunch, with a 5 µs gate placed on the photon signal from laser-ion bunch interactions to reduce background from non-resonant scattered photons by a factor of 4×10^4. Due to the relatively fast release of Zn from the target [23], the background was further suppressed by limiting ISCOOL accumulation and release cycles to 600 ms after each proton pulse.

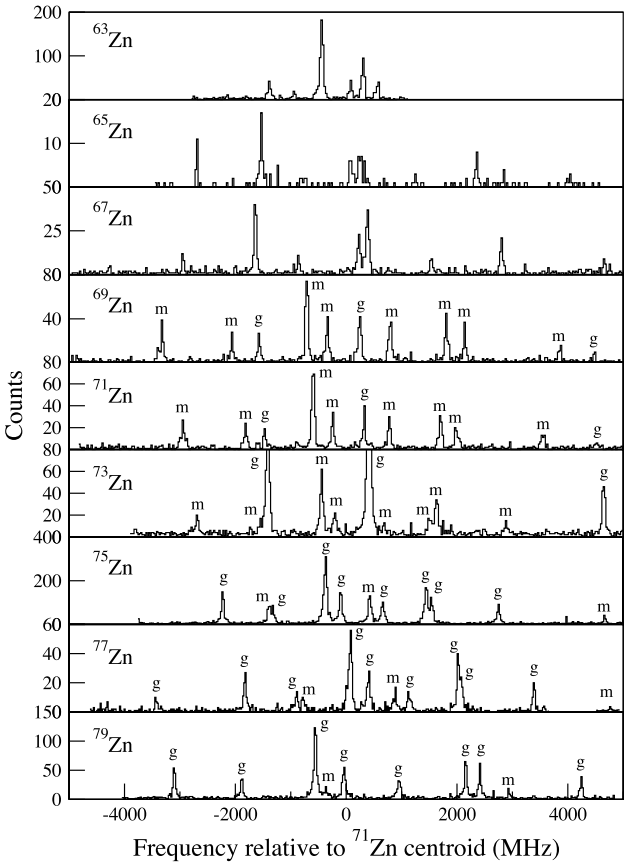

Fig. 1. Hyperfine spectra for $^{63-79}$Zn from the 4s4p $^3P_2^o \rightarrow$ 4s5s $^3S_1$ transition, including isomeric structures. See [13] for the full hyperfine spectrum of ^{79,79m}Zn.

3. Experimental results

Optical spectra for $^{63-79}$Zn are shown in Fig. 1 for the 481.2 nm line. A full hfs was fitted to each experimental spectrum with a χ^2-minimisation fitting program to obtain the magnetic dipole, A, and electric quadrupole, B, hfs constants [24]. A slightly asymmetric line shape occurs from energy losses, either by the population of higher levels in the charge exchange process or by additional collisions. The line shape has been modelled using the

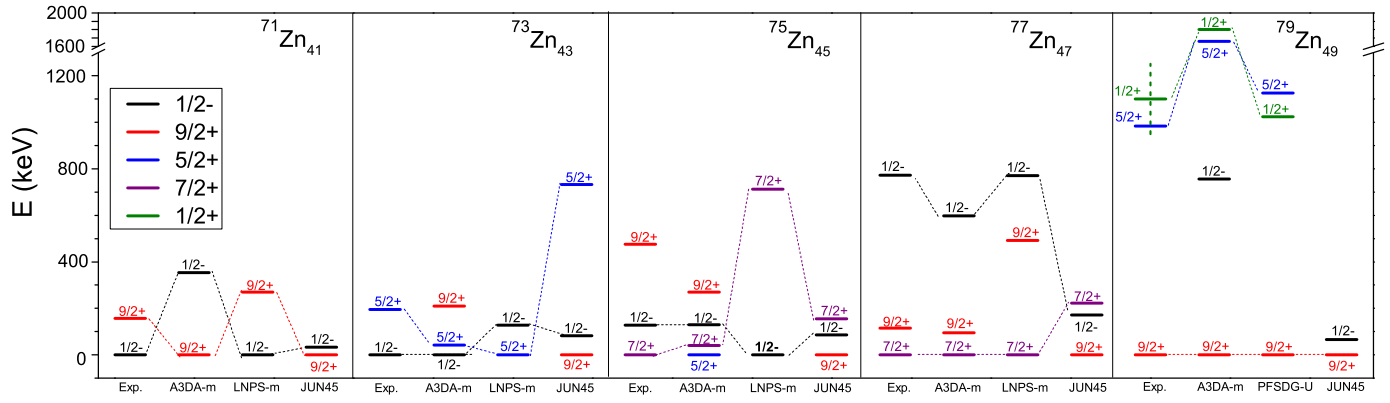

Fig. 2. Low energy spectra of Zn isotopes from $N = 41$–49 are compared to the predictions from shell–model interactions. The change in energy of the confirmed ground and isomeric states are highlighted by dotted lines. The vertical dashed line in the $1/2^+$ isomeric state of ^{79}Zn represents the error on the measured energy.

Table 1
Spins and hfs constants of the upper and lower states of the 481.2 nm line, for ground and isomeric states of $^{63-79}$Zn. Note that $B(^3S_1) \approx 0$.

A	N	I	$A(^3S_1)$ (MHz)	$A(^3P_2^o)$ (MHz)	$B(^3P_2^o)$ (MHz)
63	33	3/2	−676.9(8)	−286.0(13)	+60(4)
65	35	5/2	+1114.0(23)	+467.6(10)	−7(6)
67	37	5/2	+1266.5(18)	+531.2(11)	+41(7)
69	39	1/2	+4033(9)	+1691(5)	–
69^m	39	9/2	−933.7(4)	−392.1(2)	−113(4)
71	41	1/2	+3987(5)	+1675(3)	–
71^m	41	9/2	−844.5(9)	−354.3(3)	−76(5)
73	43	1/2	+4044.0(27)	+1696.9(16)	–
73^m	43	5/2	−1233.9(14)	−518.2(9)	+125(6)
75	45	7/2	−815.4(6)	−342.3(4)	+48(4)
75^m	45	1/2	+4034(6)	+1695.5(29)	–
77	47	7/2	−938.1(7)	−393.8(4)	+141(5)
77^m	47	1/2	+4063(10)	+1708(5)	–
79	49	9/2	−955.0(6)	−400.6(3)	+116(5)
79^m	49	1/2	−7362(6)	−3093(4)	–

high-statistics spectrum of an even-A isotope and was fixed in fitting the spectra of all odd-A isotopes [25].

Unambiguous spin assignments could be made for all nuclei and isomers as only a single spin value reproduces all hfs peak spacings simultaneously. The resulting spin assignments and hyperfine constants are shown in Table 1. Moments are calibrated relative to those of ^{67}Zn by using the hyperfine constants $A(^3P_2^o) = +531.987(5)$ MHz (given a negligible hyperfine anomaly [26]) and $B(^3P_2^o) = +35.806(5)$ MHz [27]. We used the nuclear magnetic dipole moment $\mu = +0.875479(9)\ \mu_N$ [28] and an updated value for the quadrupole moment, based on new calculations of the electric field gradient (EFG) for the 4s4p $^3P^o_{1,2}$ states. Applying both the non-relativistic Hartree–Fock and fully relativistic Dirac–Hartree–Fock multiconfiguration methods [29], using respectively ATSP [30] and GRASP [31] atomic structure codes, different electron correlation models were investigated and their consistency checked between the non-relativistic and relativistic approaches. From this study, a set of A, EFG and Q_s values are produced [32] from which we derived a quadrupole moment value of $Q_s = +0.122(10)$ b. Recently the EFG of Zn in solid Zn has been recalculated using a hybrid Density Functional Theory approach [33]. Combining this value with the experimental quadrupole coupling constants measured by Potzel et al. [34], and corrected for thermal effects, a new quadrupole moment value for ^{67}Zn g.s., $Q_s = +0.122(5)$ b, is determined in [33]. Although this value perfectly agrees with the present atomic estimation, the claimed error bars appear to be very optimistic, taking the general uncertainty of the DFT functional developments into account. We therefore adopted the reference value $Q_s = +0.122(10)$ b for the g.s. of ^{67}Zn. All extracted moments are shown in Table 2.

4. Nuclear spins of ground and isomeric states

In Fig. 2 we present the experimental ground and isomeric states in $^{71-79}$Zn, for which firm spin-assignments have been made. The assigned parities are based on the measured magnetic moments, as discussed in the next section.

When filling the $\nu g_{9/2}$ orbital from $N = 41$ onwards, a g.s. spin $I = 9/2$ would be expected for the odd-Zn isotopes, in the case that no deformation or correlations are present. This is not the case for any of these isotopes, except for the one-neutron–hole isotope ^{79}Zn. This is evidence for the magic nature of the $N = 50$ shell and suggests that the lighter Zn isotopes exhibit significant correlations in their ground states, leading to non-trivial g.s. spins. For ^{71,73}Zn, the g.s. spin-parity $1/2^-$ that was tentatively assigned previously [15] is confirmed. The $9/2^+$ state appears to be isomeric in ^{71}Zn, and has not yet been observed in ^{73}Zn. Instead, a $5/2^+$ isomeric state is observed [18]. In ^{75,77}Zn, the g.s. spin is $7/2^+$ and the $1/2^-$ becomes now a long-lived isomeric state. Finally, in ^{79}Zn, having 49 neutrons, the g.s. spin is the $9/2^+$ expected from a non-interacting shell model picture with a hole in the $\nu g_{9/2}$ orbital. A long-lived isomeric state with spin-1/2 has been established in this isotope, but its large negative magnetic moment excluded a negative parity for this isomer [13].

In Fig. 2 we compare the lowest energy levels in odd-A Zn isotopes with large-scale shell–model calculations in different model spaces and using different interactions. The simplest model space starts from a ^{56}Ni core, with protons and neutrons in the $f_{5/2}$, p and $g_{9/2}$ orbits. Two effective interactions are available in this model space, JUN45 [35] and jj44b [3]. This model space is extended to include proton excitations from $\pi f_{7/2}$ across $Z = 28$ and neutron excitations across $N = 50$ into the $\nu d_{5/2}$ orbital. Two interactions are available in this extended model space: the modified A3DA interaction (A3DA-m) [36] in the Monte Carlo Shell-Model (MCSM) [37] framework and the modified LNPS interaction (LNPS-m) that is used with the ANTOINE code [38]. To understand the structure of the newly found positive parity isomer in ^{79}Zn, we use the recently developed PFSDG-U interaction [39] in the proton pf and neutron sdg valence space.

As can be seen in Fig. 2, none of the calculations reproduces correctly the energy level ordering of all ground and isomeric states in these isotopes. In the calculations with a ^{56}Ni core (JUN45) the g.s. spin is predicted to be $9/2^+$ for all isotopes. By opening the proton shell to include excitations from the $\pi f_{7/2}$ orbital across $Z = 28$, as well as excitations to the $\nu d_{5/2}$ orbital

Table 2
Nuclear magnetic dipole moments, μ, and spectroscopic quadrupole moments, Q_s, calculated from experimental data are compared to JUN45, LNPS-m and A3DA-m shell–model calculations.

A	I^π	μ_{expt} (μ_N)	μ_{JUN45} (μ_N)	μ_{LNPS-m} (μ_N)	μ_{A3DA-m} (μ_N)	$Q_{s,expt}$ (b)	$Q_{s,JUN45}$ (b)	$Q_{s,LNPS-m}$ (b)	$Q_{s,A3DA-m}$ (b)
63	$3/2^-$	−0.282(1)	−0.256	−0.18	+0.110	+0.20(2)	+0.240	+0.19	+0.209
65	$5/2^-$	+0.7695(16)	+0.938	+0.77	+1.027	−0.024(15)	−0.049	−0.036	+0.013
67	$5/2^-$	+0.875479(9)[a]	+1.008	+1.31	+1.309	+0.122(10)[a]	+0.128	+0.10	+0.219
69	$1/2^-$	+0.557(2)	+0.463	+0.47	+0.404	–	–	–	–
69^m	$9/2^+$	−1.1613(7)	−1.156	−1.27	−1.306	−0.39(3)	−0.410	−0.40	−0.435
71	$1/2^-$	+0.551(1)	+0.456	+0.48	+0.482	–	–	–	–
71^m	$9/2^+$	−1.049(1)	−1.159	−1.10	−1.434	−0.26(3)	−0.284	−0.22	−0.264
73	$1/2^-$	+0.5585(5)	+0.451	+0.50	+0.521	–	–	–	–
73^m	$5/2^+$	−0.8527(14)	−0.984	−0.81	−0.543	+0.43(4)	+0.281	+0.48	+0.420
75	$7/2^+$	−0.7887(9)	−0.915	−0.88	−0.614	+0.16(2)	+0.070	+0.20	+0.055
75^m	$1/2^-$	+0.5580(9)	+0.445	+0.51	+0.509	–	–	–	–
77	$7/2^+$	−0.9074(1)	−0.876	−1.04	−0.964	+0.48(4)	+0.421	+0.60	+0.487
77^m	$1/2^-$	+0.562(2)	+0.450	+0.50	+0.537	–	–	–	–
79	$9/2^+$	−1.1866(10)	−1.185	−1.49	−1.508	+0.40(4)	+0.356	+0.546	+0.367
79^m	$1/2^+$	−1.018(1)	–	−0.741	−0.603	–	–	–	–

[a] To calibrate across the isotope chain the nuclear moments of ^{67}Zn are used as references, with μ and Q_s taken from [28] and this work respectively, with details given in [32]. Precise hyperfine constants $A(^3P_2)$ and $B(^3P_2)$ [27] are used.

(A3DA-m and LNPS-m) the agreement becomes better for ^{77}Zn. However, for the less exotic isotopes the level ordering is still not well reproduced. These interactions predict a positive-parity $1/2^+$ level in ^{79}Zn, although it appears at 1.8 and 1.5 MeV respectively, well above the experimental energy of 1.10(15) MeV [14]. The magnetic moment of this level motivated a further extension of the model space, as realized in the PFSDG-U interaction. In this extended model space an isomeric $1/2^+$ level is found at the experimental energy.

5. Ground and isomeric state g-factors and wave functions

In the f_5pg_9 model space used for JUN45 and jj44b, we use $g_s^{eff} = 0.7g_s^{free}$ for magnetic moment calculations, and effective charges $e_p^{eff} = 1.5e$, $e_n^{eff} = 1.1e$ [35]. These interactions were used in our previous work on the nuclear moments and spins of the Cu and Ga ground states [40,3], reproducing these observables rather well. The LNPS-m and A3DA-m interactions start from a ^{40}Ca core and include also the $d_{5/2}$ orbital, thus using a fpg_9d_5 model space. The neutron $f_{7/2}$ orbit is blocked for the LNPS-m calculations, but this has no influence on the spectroscopy of the neutron-rich ($N > 38$) isotopes. Free g-factors can be applied in this extended model space. Furthermore, the effective neutron charge can be reduced to $e_n^{eff} = 0.46e$ because of the inclusion of the $\nu d_{5/2}$ orbital, while the proton charge is taken as $e_p^{eff} = 1.31e$ [38]. The nuclear moments have been calculated for the lowest lying energy level with the confirmed spin assignment.

The nuclear magnetic moment provides a sensitive probe of the wave function of the state. By comparing the measured magnetic moments, and more specifically the corresponding g-factor ($g = \mu/I$) to the effective SP values of nearby orbitals, the leading contributions to the wave functions can be deduced (Fig. 3). These values are also compared to the predictions of the shell–model interactions, from which we can extract the calculated main contribution in the wave function.

The experimental g-factors for the $1/2^-$ ground states of ^{69,71,73}Zn and the isomeric states in ^{75,77}Zn are in good agreement with the effective SP value for the $\nu p_{1/2}$ orbit. The $(\nu p_{1/2})^1$ led wave function configuration for these states is confirmed by the calculations in the f_5pg_9 model space that predict a >50% contribution from a $\nu p_{1/2}$ hole configuration for the ground states and >60% for the isomers. The calculated magnetic moments appear to systematically underestimate the measured values of the $1/2^-$ states. Further theoretical investigations are needed to understand this.

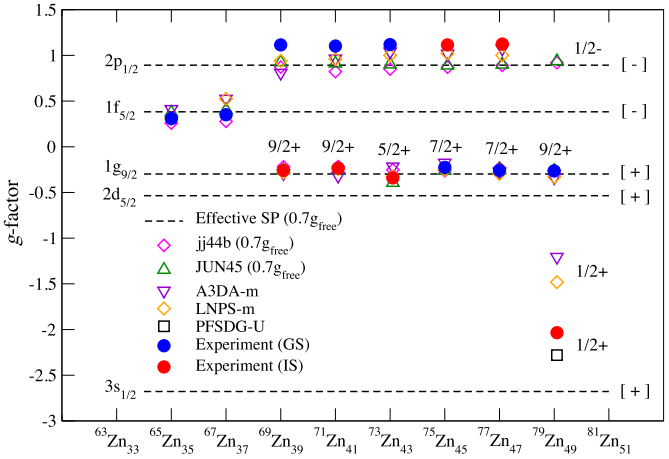

Fig. 3. Measured g-factors of the ground and isomeric states of $^{65-79}$Zn. The observed results are compared to the effective SP values (parity in brackets) and predictions of shell–model interactions (see text for details).

The ground states of ^{65,67}Zn ($N = 35, 37$) both have spin $5/2^+$ and their g-factor is in good agreement with that for an unpaired neutron configuration in the $\nu f_{5/2}$ orbital. The high-spin states in the $^{69-79}$Zn isotopes, having spins $9/2^+$, $5/2^+$ and $7/2^+$, all have a g-factor that is very close to that for an unpaired neutron configuration in the $\nu g_{9/2}$ orbital, suggesting this is the leading term in their wave function.

For the isomeric $9/2^+$ states in ^{69,71}Zn and the $9/2^+$ g.s. in ^{79}Zn, a single unpaired $g_{9/2}$ neutron configuration is expected to dominate the wave function. That is confirmed by the large-scale shell–model calculations from JUN45 and jj44b, which predict this configuration to have the largest contribution indeed: about 50% in ^{69}Zn ($N = 39$), 40% in ^{71}Zn ($N = 41$) and nearly 100% in ^{79}Zn ($N = 49$). The excellent agreement of the calculated magnetic moments with the observed value for the ^{79}Zn g.s. with all interactions (Table 2), illustrates the persistence of $N = 50$ as a shell gap. Also the values for the $7/2^+$ ground states in ^{75,77}Zn are well reproduced by all large scale shell–model calculations. The leading term in their wave function is a seniority-3 $\nu(g_{9/2})^3_{7/2}$ configuration, which makes up roughly half of the wave function in ^{75}Zn and ^{77}Zn.

The $5/2^+$ isomeric state in ^{73}Zn also has a g-factor that agrees well with the value for an unpaired $g_{9/2}$ neutron configuration. Note that this $5/2^+$ g-factor does not agree with that of a $\nu d_{5/2}$

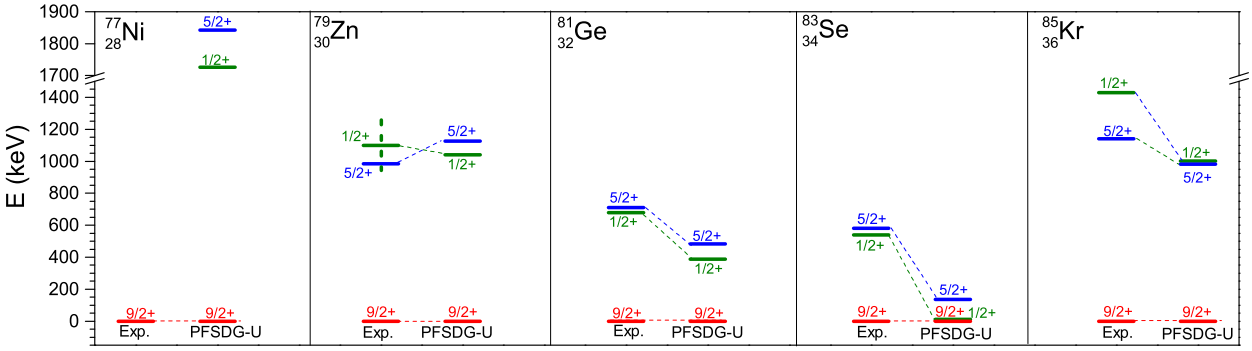

Fig. 5. Positive-parity levels in $N = 49$ isotopes due to neutron excitations across $N = 50$, compared the calculated levels with the PFSDG-U interaction. The vertical dashed line in the $1/2^+$ isomeric state of ^{79}Zn represents the error on the measured energy.

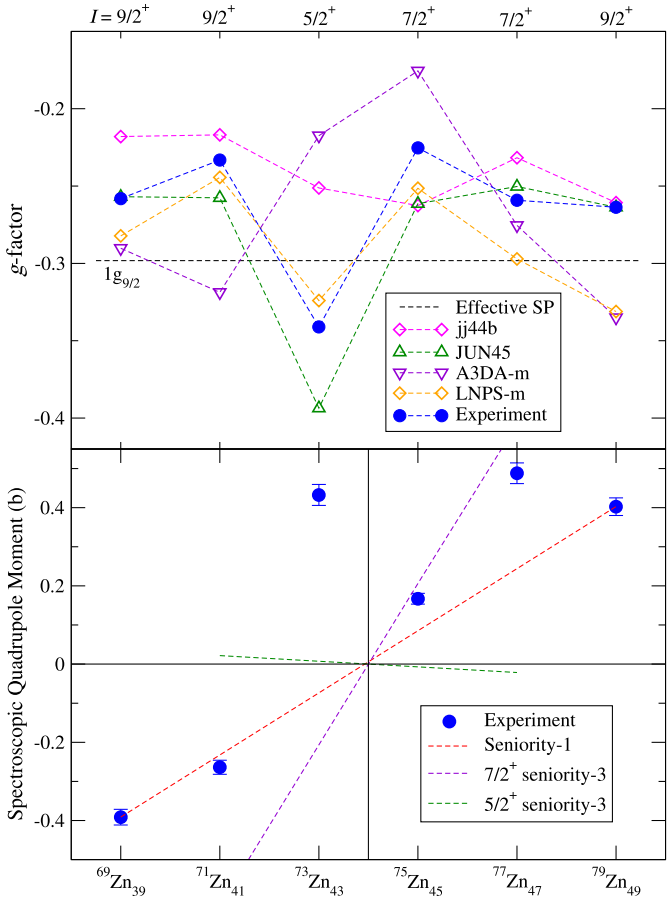

Fig. 4. (a) High-spin state g-factors in relation to the effective SP value of $g_{\rm eff}(\nu g_{9/2})$. (b) Measured spectroscopic quadrupole moments of the high spin states of Zn isotopes compared to the expected values for a seniority-1 $(g_{9/2})^n$ configuration and the spin-$7/2^+$ and $5/2^+$ seniority-3 configurations. (For interpretation of the references to colour in this figure, the reader is referred to the web version of this article.)

SP configuration. This excludes that this $5/2^+$ isomeric state is an intruder isomer, dominated by a neutron excited into the $\nu d_{5/2}$ orbital. The fact that its g-factor is somewhat lower than that of the other high-spin states suggests that some admixture with such a configuration cannot be excluded. In Fig. 4a, the high-spin g-factors are presented on a smaller scale, in order to better see how well each of the calculations agrees with the data. The divergence of predictions from the LNPS-m and A3DA-m interactions from experiment towards $N = 50$ while JUN45 and jj44b converge hints at the persistence of the $Z = 28$ and $N = 50$ shell gaps. All

Table 3
Calculated energies (MeV) and electromagnetic moments μ (μ_N) and Q_s (b) for ^{79}Zn and ^{81}Ge using the PFSDG-U interaction. The same effective charges are used as for LNPS-m.

^AZ	I^π	E	$\mu_{\rm exp}$	$\mu_{\rm bare}/\mu_{\rm quenched}$	$Q_{s,\rm exp}$	Q_s
^{79}Zn	$9/2^+$	0.0	−1.1866	−1.03/−1.10	+0.40	+0.42
	$1/2^+$	1.03	−1.018	−1.14/−0.91	–	–
^{81}Ge	$9/2^+$	0.0	–	−0.90/−0.95	–	+0.60
	$1/2^+$	0.31	–	−1.15/−0.94	–	–

interactions predict a very fragmented wave function for the $5/2^+$ isomeric state in ^{73}Zn, with the largest contribution in JUN45 being less than 10%.

For the isomeric state in ^{79}Zn, the model space limitations of the JUN45 and jj44b interactions prevent any predictions for the positive parity $1/2^+$ state. The spin and positive parity of this level were tentatively assigned in [14] and firmly established by [13], based on its strong negative g-factor, which is incompatible with a $p_{1/2}$ hole configuration (see Fig. 3). The larger model space of the LNPS-m and A3DA-m interactions consider excitations across the $N = 50$ shell closure into the $\nu d_{5/2}$ orbit only. In this model space, a $1/2^+$ level is predicted at 1.8 and 1.5 MeV respectively, with g-factors $g_{\rm A3DA-m} = -1.206$ and $g_{\rm LNPS-m} = -1.482$, closer to the observed value, $g_{\rm exp} = -2.038$, but still not in agreement. In [13], a 1p–2h neutron excitation to a positive parity spin-1/2 state is suggested, with a large part of the wave function dominated by a single neutron in the $s_{1/2}$ orbit.

A new shell model interaction has been developed, suitable to calculate levels in isotopes around $N = 50$ with protons limited to the pf shell and neutrons to the sdg space [39], including all spin–orbit partners (allowing the use of free g-factors). Thus the interaction is not suited to calculate levels in which neutrons in the pf orbits play an important role (such as the $1/2^-$ isomeric states in ^{75,77}Zn). Therefore, we limit the calculations to the $N = 49$ isotones with protons in the pf shell, where positive-parity intruder orbits have been observed between $Z = 38$ and $Z = 30$. In Fig. 5 we compare the calculated lowest positive parity $9/2^+$, $1/2^+$ and $5/2^+$ levels in ^{85}Kr, ^{83}Se, ^{81}Ge, ^{79}Zn and ^{77}Ni to the experimental data. The energies for these intruder levels are well reproduced for ^{79}Zn, given typical shell–model uncertainties (a few 100 keV) on energy predictions. For ^{77}Ni, these intruder levels are predicted close to 2 MeV, suggesting a rather good doubly-magic nature for ^{78}Ni. For the heavier isotones they appear 200 to 500 keV too low, which needs some further investigation.

The $1/2^+$ state appears to be isomeric in ^{79}Zn and ^{81}Ge [41], and the intruder nature of this state is firmly established via its magnetic moment. Indeed, excellent agreement is observed between the calculated and observed magnetic moment of the intruder state in ^{79}Zn (Table 3). In Fig. 6 we represent the normal-

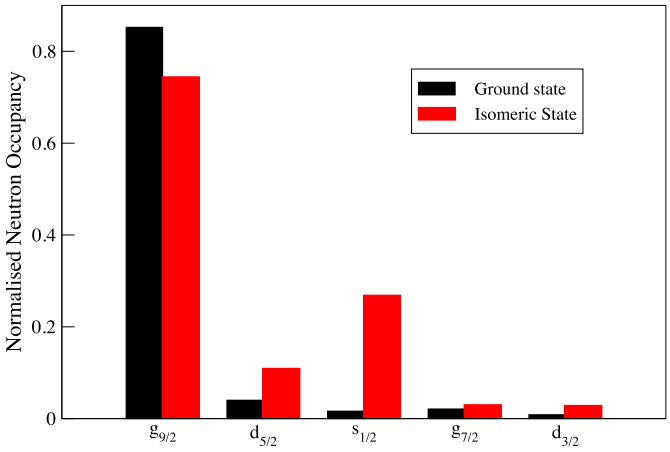

Fig. 6. Neutron occupancy normalised to the maximum orbital nucleon number for the ground and isomeric states in ^{79}Zn from the PFSDG-U interaction.

ized neutron occupancy in all *sdg* levels. The g.s. wave function is dominated by a single neutron hole in the $g_{9/2}$ orbit (50%), but a significant amount of neutron excitations into the *sd* space are observed for the isomeric state. That leads to a better agreement with the experimental magnetic and quadrupole moment compared to the LNPS-m calculations. The isomeric level has a large occupancy of the $s_{1/2}$ level, but also more np–nh excitations into the $d_{5/2}$ orbital as well as the higher *gd* orbits. The main component in the isomeric wave function is found to be indeed of a 1p–2h nature (40%).

6. Quadrupole moments of ground and isomeric states

The quadrupole moments of the high-spin states, shown in Fig. 4b, are able to shed further light on the single particle structure as well as collectivity and structural changes across the isotope chain as the $\nu g_{9/2}$ orbit is filled. In Table 2, the A3DA-m interaction is shown to most accurately predict the measured quadrupole moments of neutron rich isotopes from $^{69-79}$Zn, except for the g.s. of ^{75}Zn.

Already starting from ^{69}Zn, the neutrons gradually fill the $g_{9/2}$ orbital. In general the quadrupole moment should reflect the nature of a single $g_{9/2}$ neutron particle in ^{69}Zn and single $g_{9/2}$ neutron hole in ^{79}Zn, as discussed for the magnetic moments measured in this work. In Fig. 4b it can be seen that the 1p configuration for the isomeric state in ^{69}Zn has indeed the opposite quadrupole moment of the 1h configuration for the g.s. of ^{79}Zn. The quadrupole moments for the seniority-1 $(\nu g_{9/2})^n$ configurations with spin-9/2 (^{69,71,79}Zn) follow the expected linear increase, crossing zero in the middle of the shell [42] (red dashed line of Fig. 4b) which corresponds to $A = 74$ in the present case. The experimental magnetic moments of the $7/2^+$ states in ^{75,77}Zn show a seniority-3 $\nu(g_{9/2})^3_{7/2^+}$ configuration, explaining why the their quadrupole moments do not follow the straight line of the seniority-1 cases.

An estimate of the quadrupole moments of the $7/2^+$ seniority-3 states can be obtained using the effective single-particle quadrupole moment observed in the seniority-1 cases, $Q_{sp} = \langle J|\hat{Q}|J\rangle$, the applicable coefficients of fractional parentage [43] and the relation [44,45],

$$\langle J^n(I) \mid \widehat{Q} \mid J^n(I)\rangle = \frac{2J+1-2n}{2J+1-2\nu}\nu \sum_{J_1}(-1)^{J_1+J+I}(\mathrm{cfp})^2 \times (2I+1)\begin{Bmatrix} J & I & J_1 \\ I & J & 2 \end{Bmatrix}\langle J|\widehat{Q}|J\rangle \quad (1)$$

in which the quadrupole moment of a state with n particles in an orbit and seniority ν is linked to the Q_{sp} via the coefficients of fractional parentage, $\mathrm{cfp} = [J^{n-1}(\nu_1, J_1), J; I|\}J^n\nu I]$ [44]. Predictions for the seniority-3 $I = 7/2^+$ (violet dashed line) and $I = 5/2^+$ states (green dashed line) based on eq. (1) are presented in Fig. 4b. The experimental values for ^{75,77}Zn are observed to follow this trend.

The larger quadrupole moment of $5/2^+$ state of ^{73m}Zn does not coincide with the seniority-3 $5/2^+$ prediction, indicating substantial deformation. This confirms the conclusions from earlier beta-decay studies [15] and transfer reaction studies [46], where the observed low-energy spectra of ^{73}Zn were interpreted as a more strongly deformed prolate structures ($\beta \approx +0.2$) in ^{73}Zn. This result, along with the increase of configuration mixing at ^{73m}Zn mentioned above, witnessed both in its magnetic moment and its quadrupole moment, therefore signals a rapid shape transition at $N = 43$ in the Zn isotopes. A low-energy Coulomb excitation study of zinc isotopes at REX-ISOLDE supports this conclusion. Here a sudden lowering of 2^+ states at $N = 40$ and an increase in B(E2$\downarrow$) strength towards $N = 44$ was associated with an increase in collectivity due to proton–neutron correlations and a weakening of the sub-shell closure [47,48]. An onset of collectivity is also observed in the quadrupole moments of odd-A Ga isotopes when $N > 40$ [3], while no such increase in collectivity is observed in the quadrupole moments of Cu isotones [40]. Therefore, Zn isotopes are considered to lie within a transitional region between spherical Ni and deformed Ge nuclei [49].

7. Conclusion

In summary, the nuclear spins, magnetic dipole moments and electric quadrupole moments have been determined for the ground and isomeric states in $^{63-79}$Zn by means of collinear laser spectroscopy. Exactly one long-lived ($t_{1/2} > 10$ ms) isomeric state has been observed in all odd-A Zn isotopes from $N = 39$–49. This has provided an insight into the neutron level systematics as the $N = 50$ shell closure is approached.

The magnetic dipole moments of ground and isomeric states have been compared to a variety of large-scale shell–model calculations in different model spaces. All states up to ^{79}Zn (except for the $1/2^+$ isomeric level) are well described with interactions assuming a ^{56}Ni core and neutrons limited to the *pf* and $g_{9/2}$ orbits. Extending the model space both for proton excitations across $Z = 28$ and neutron excitations across $N = 50$ does not significantly improve the agreement with experiment, with their high-spin g-factors diverging from the experimental values for $N = 45$–49 suggesting the preservation of these shell gaps when approaching ^{78}Ni.

For the $1/2^+$ intruder isomer, a newly developed shell–model interaction in the *pf*+*sdg* model space is needed to reproduce the magnetic dipole moment of ^{79m}Zn, which lies outside the f_5pg_9 and fpg_9d_5 model spaces. The PFSDG-U interaction suggests a leading wave function configuration formed by a 1p–2h excitation from $\nu g_{9/2}$ to $\nu 3s_{1/2}$, consistent with the spin-parity of the isomeric state as $1/2^+$. A similar isomeric intruder level has been suggested in ^{81}Ge [41] and a future magnetic moment measurement should confirm its 1p–2h intruder nature. Also in ^{80}Ga a low-lying short-lived intruder 0^+ state has been inferred from β-decay studies [50]. Thus further studies to establish the deformation of these proposed shape-coexisting states are needed.

The quadrupole moments reveal a strong onset of collectivity from ^{71m}Zn to ^{73m}Zn, where the deviation of the quadrupole moment from the seniority-3 $5/2^+$ prediction indicates substantial deformation at $N = 43$. The measured quadrupole moments are

described most accurately by the A3DA-m interaction, but in general they are well reproduced by all shell–model interactions.

Acknowledgements

The support and assistance from the ISOLDE technical group are gratefully acknowledged. This work was supported by the IAP-project P7/12, the FWO-Vlaanderen, GOA grant 15/010 from KU Leuven, the BMBF Contracts Nos. 05P15RDCIA, the Max-Planck Society, the Science and Technology Facilities Council, and the EU FP7 via ENSAR No. 262010. The atomic calculations of EFGs were supported from the European Regional Development Fund in the framework of the Polish Innovation Economy Operational Program (contract no. POIG.02.01.00-12-023/08). PJ acknowledges support from the Swedish Research Council under contract 2015-04842. The Monte Carlo Shell-Model calculations were performed on K computer at RIKEN AICS (hp150224, hp160211). This work was supported in part by the HPCI Strategic Program (the origin of matter and the universe) and "Priority Issue on Post-K computer" (Elucidation of the Fundamental Laws and Evolution of the Universe) from MEXT and JICFuS.

References

[1] O. Sorlin, et al., Phys. Rev. Lett. 88 (2002) 092501.
[2] M.L. Bissell, et al., Phys. Rev. C 93 (2016) 064318.
[3] B. Cheal, et al., Phys. Rev. Lett. 104 (2010) 252502.
[4] P.T. Hosmer, H. Schatz, et al., Phys. Rev. Lett. 94 (2005) 112501.
[5] K.T. Flanagan, et al., Phys. Rev. Lett. 103 (2009) 142501.
[6] T. Otsuka, et al., Phys. Rev. Lett. 95 (2005) 232502.
[7] M.G. Porquet, O. Sorlin, Phys. Rev. C 85 (2012) 014307.
[8] K. Sieja, F. Nowacki, Phys. Rev. C 85 (2012) 051301.
[9] S. Baruah, et al., Phys. Rev. Lett. 101 (2008) 262501.
[10] J. Hakala, et al., Phys. Rev. Lett. 101 (2008) 052502.
[11] Z.Y. Xu, et al., Phys. Rev. Lett. 113 (2014) 032505.
[12] Y. Shiga, et al., Phys. Rev. C 93 (2016) 024320.
[13] X.F. Yang, et al., Phys. Rev. Lett. 116 (2016) 182502.
[14] R. Orlandi, et al., Phys. Lett. B 740 (2015) 298–302.
[15] M. Huhta, et al., Phys. Rev. C 58 (1998) 3187–3194.
[16] E. Runte, et al., Nucl. Phys. A 441 (1985) 237–260.
[17] S.V. Ilyushkin, et al., Phys. Rev. C 80 (2009) 054304.
[18] S.V. Ilyushkin, et al., Phys. Rev. C 83 (2011) 014322.
[19] A.C. Mueller, et al., Nucl. Phys. A 403 (1983) 234.
[20] R. Catherall, et al., Nucl. Instrum. Methods B 204 (2003) 235–239.
[21] B.A. Marsh, et al., Hyperfine Interact. 196 (2010) 129–141.
[22] E. Mané, et al., Eur. Phys. J. A 42 (2009) 503–507.
[23] U. Köster, et al., AIP Conf. Proc. 798 (2005) 315–326.
[24] P. Campbell, et al., Prog. Part. Nucl. Phys. 86 (2016) 127–180.
[25] N. Bendali, et al., J. Phys. B 19 (1986) 233.
[26] N. Frömmgen, et al., Eur. Phys. J. D 69 (2015) 164.
[27] A. Lurio, Phys. Rev. 126 (1962) 1768–1773.
[28] N. Stone, in: International Nuclear Data Committee, vol. 0658, 2014, pp. 1–171.
[29] C.F. Fischer, et al., J. Phys. B, At. Mol. Opt. Phys. 49 (2016) 182004.
[30] C.F. Fischer, et al., Comput. Phys. Commun. 176 (2007) 559–579.
[31] P. Jönsson, et al., Comput. Phys. Commun. 184 (2013) 2197–2203.
[32] J. Bieroń, et al., in preparation.
[33] H. Haas, et al., Europhys. Lett. 117 (2017) 62001.
[34] W. Potzel, et al., Hyperfine Interact. 12 (1982) 135–141.
[35] M. Honma, et al., Phys. Rev. C 80 (2009) 064323.
[36] Y. Tsunoda, T. Otsuka, N. Shimizu, et al., Phys. Rev. C 89 (2014) 031301.
[37] T. Otsuka, Nucl. Phys. A 693 (2001) 383–393.
[38] S.M. Lenzi, et al., Phys. Rev. C 82 (2010) 054301.
[39] F. Nowacki, et al., Phys. Rev. Lett. 117 (2016) 272501.
[40] P. Vingerhoets, et al., Phys. Rev. C 82 (2010) 064311.
[41] P. Hoff, B. Fogelberg, Nucl. Phys. A 368 (1981) 210–236.
[42] G. Neyens, Rep. Prog. Phys. 66 (2003) 633–689.
[43] B. Bayman, A. Lande, Nucl. Phys. 77 (1966) 1–80.
[44] A. de Shalit, I. Talmi, Nuclear Shell Theory, Elsevier, 1963.
[45] D.T. Yordanov, et al., Phys. Rev. Lett. 110 (2013) 192501.
[46] M. Bernas, et al., Nucl. Phys. A 413 (1984) 363–374.
[47] J. Van De Walle, et al., Phys. Rev. C 79 (2009) 014309.
[48] O. Perru, et al., Phys. Rev. Lett. 96 (2006) 232501.
[49] S. Leenhardt, et al., Eur. Phys. J. A 14 (2002) 1–5.
[50] A. Gottardo, et al., Phys. Rev. Lett. 116 (2016) 182501.